


Article

A First Attempt to Combine NIRS and Plenoptic Cameras for the Assessment of Grasslands Functional Diversity and Species Composition

Simon Taugourdeau ^{1,2,*} , Mathilde Dionisi ^{1,2}, Mylène Lascoste ^{1,2}, Matthieu Lesnoff ^{1,2}, Jean Marie Capron ^{1,2}, Frédéric Borne ^{3,4}, Philippe Borianne ^{3,4} and Lionel Julien ^{1,2}

- ¹ CIRAD UMR SELMET, F-34090 Montpellier, France; mathilde.dionisi@cirad.fr (M.D.); mylenelacoste@gmail.com (M.L.); matthieu.lesnoff@cirad.fr (M.L.); jean-marie.capron@inrae.fr (J.M.C.); lionel.julien@cirad.fr (L.J.)
- ² UMR SELMET INRAE CIRAD, Institut Agro University of Montpellier, F-34090 Montpellier, France
- ³ CIRAD UMR AMAP, F-34090 Montpellier, France; frederic.borne@cirad.fr (F.B.); philippe.borianne@cirad.fr (P.B.)
- ⁴ UMR AMAP, CIRAD, CNRS, IRD INRAE, University of Montpellier, F-34090 Montpellier, France
- * Correspondence: simon.taugourdeau@cirad.fr



Citation: Taugourdeau, S.; Dionisi, M.; Lascoste, M.; Lesnoff, M.; Capron, J.M.; Borne, F.; Borianne, P.; Julien, L. A First Attempt to Combine NIRS and Plenoptic Cameras for the Assessment of Grasslands Functional Diversity and Species Composition. *Agriculture* **2022**, *12*, 704. <https://doi.org/10.3390/agriculture12050704>

Academic Editors: Dionissios Kalivas, Christos Chalkias, Thomas Alexandridis, Konstantinos X. Soulis and Emmanouil Psomiadis

Received: 14 April 2022

Accepted: 15 May 2022

Published: 17 May 2022

Publisher's Note: MDPI stays neutral with regard to jurisdictional claims in published maps and institutional affiliations.



Copyright: © 2022 by the authors. Licensee MDPI, Basel, Switzerland. This article is an open access article distributed under the terms and conditions of the Creative Commons Attribution (CC BY) license (<https://creativecommons.org/licenses/by/4.0/>).

Abstract: Grassland represents more than half of the agricultural land. Numerous metrics (biomass, functional trait, species composition) can be used to describe grassland vegetation and its multiple functions. The measures of these metrics are generally destructive and laborious. Indirect measurements using optical tools are a possible alternative. Some tools have high spatial resolutions (digital camera), and others have high spectral resolutions (Near Infrared Spectrometry NIRS). A plenoptic camera is a multifocal camera that produces clear images at different depths in an image. The objective of this study was to test the interest of combining plenoptic images and NIRS data to characterize different descriptors of two Mediterranean legumes mixtures. On these mixtures, we measured biomass, species biomass, and functional trait diversity. NIRS and plenoptic images were acquired just before the field measurements. The plenoptic images were analyzed using Trainable Weka Segmentation ImageJ to evaluate the percentage of each species in the image. We calculated the average and standard deviation of the different colors (red, green, blue reflectance) in the image. We assessed the percentage of explanation of outputs of the images and NIRS analyses using variance partition and partial least squares. The biomass *Trifolium michelianum* and *Vicia sativa* were predicted with more than 50% variability explained. For the other descriptors, the variability explained was lower but nevertheless significant. The percentage variance explained was nevertheless quite low, and further work is required to produce a useable tool, but this work already demonstrates the interest in combining image analysis and NIRS.

Keywords: image segmentation; legumes; Mediterranean grassland; *Trifolium*; *Vicia*; *Medicago*; *Avena*

1. Introduction

Grazing land represents a large part of the worldwide agricultural areas [1]. Grassland vegetation is diverse within or between plots. Grassland vegetation is characterized using different descriptors depending on the research area. In grassland agronomy and animal sciences, biomass is generally the main used descriptor. The quality of the forage for animal nutrition is assessed by a set of descriptors that include the digestibility of the forage and its protein content [2] and fiber content [3]. Other chemical components such as tannins, lipids, and micronutrients are sometimes also evaluated for forage quality [4]. In grassland ecology, the presence and abundance of plant species is usually characterized. The functional trait approach has started to be used [5] to produce a more mechanistic understanding. A functional trait is any morphological, physiological, or phenological feature measurable

at the individual scale that is linked with its functions [6]. Many functional diversity indices can be calculated from functional traits [7]. They help understand community assemblage rules [8] and the impacts of vegetation on ecosystem functions and services [9]. Each descriptor provides interesting complementary information on the different functions of grasslands.

However, measuring all these descriptors is laborious, for example, counting the number of individual plants belonging to each species in sample quadrats, measuring leaf area and mass. As many vegetation descriptors can only be measured using destructive techniques, they cannot be used to monitor vegetation dynamics over a growing season without affecting the plant cover. The destructive method is generally limited to subplots. Indirect methods can be used on a larger scale.

Alternative tools have been developed to enable indirect measurement using optical tools [10]. Some rely on the spectral properties, i.e., the infrared reflectance of the green vegetation. Infrared reflectance combined with red and sometimes blue reflectance is the inputs of many vegetation indices, including the Normalized Difference Vegetation Index (NDVI) [11]. NDVI is generally used from images obtained by remote sensing but also directly in the field with specific captors [12,13]. However, NDVI has to be calibrated with the field measures. In each case, the calibration with NDVI requires field measurements.

Spectral properties are also used with Near InfraRed Spectrometry (NIRS), which has a higher spectral resolution than the limited number of wavelengths used for NDVI. NIRS technology is now widely used to assess the nutritional quality of livestock feed (including forage) in terms of protein, dry matter, fiber, lignin content, digestibility, and crude energy [14]. The NIRS is also used to assess the ratio between two species or functional groups [15] and the evaluation of the mean value of the functional trait [16]. However, all these works were performed on dry samples inside the lab and are, therefore, destructive. Field applications of NIRS have been tested [17].

Digital cameras are also used to study the plant cover. Photography has often been used to identify and quantify the presence of weeds in a crop cover [18,19] or undesirable species such as *Rumex* sp. in grasslands [20,21]. Photography has been used to evaluate the contribution of legumes in a grass-legume mixture [22,23]. However, the focus is one of the problems with photography. Indeed, grassland vegetation, particularly natural grassland, is generally highly heterogeneous with a combination of tall and short species. With a standard camera, it is difficult to obtain a clear image of the different vegetation layers. One option is to shoot from a spot that is sufficiently high to obtain hyperfocal conditions, but this could be difficult to apply in the field, particularly in a tall and heterogeneous grassland cover.

Another option is a multifocal camera such as a plenoptic camera, also known as a light field camera, which captures the light field of a scene, i.e., the intensity of light in a scene and the direction of the light rays [24]. The resulting image can subsequently be refocused [25] to create a series of pictures with a different focus from only one shoot. The Lytro Desktop software produced by the maker of one plenoptic camera included an option to produce a clear image from the set of images by combining the different pictures.

The main aim of the study was to test the plenoptic camera and NIRS for the evaluation of several features of grassland vegetation (biomass, species composition and functional diversity). The goal was also to evaluate the complementarity between the camera and the NIRS.

We made the hypothesis that the multifocal camera (plenoptic) can produce clearer images than a classical digital camera. Furthermore, the plenoptic can produce a digital surface model that can be useful for the evaluation of vegetation metrics.

2. Material and Methods

2.1. Experimental Sites and Design

(a) Experimental sites and pedoclimatic conditions

The experimental site was the INRA Diascope experimental station in Mauguio near Montpellier, in the South of France. The climate was Mediterranean (mild winters and hot, dry summers). The average annual rainfall was 680 mm, with high variability in the quantity and distribution of rainfall [26].

The average temperature throughout the field experiment (April to July 2016) was 17.1 °C (maximum 27.2 °C, minimum 11.2 °C). Rainfall during the period of the experiment was 52 mm, and potential evapotranspiration was estimated at 343.7 mm (obtained from the meteorological station on the experimental site).

(b) Design of the plant mixtures and technical itinerary

Four 210 m² plots (each 70 m by 3 m), with 2 mixtures of grasses and legumes, were created at the beginning of April 2017. The first plot contained a mixture of *Trifolium alexandrinum*, *Medicago truncatula*, *Vicia sativa*, and *Avena sativa* (M1); the second plot contained the same species but with *Trifolium michelianum* instead of *Vicia sativa* (M2). The sowing density in each plot is detailed in Table 1.

Table 1. Composition and sowing density of the two mixtures used for the test.

	Species	Mix1 in kg·ha ^{−1}	Mix2 in kg·ha ^{−1}
Grass	<i>Avena sativa</i>	10	10
	<i>Vicia sativa</i>	15	0
Legumes	<i>Trifolium alexandrinum</i> , <i>Medicago truncatula</i>	5	5
	<i>Trifolium michelianum</i>	2.5	2.5
		0	5

To facilitate the establishment of the plant mixtures, we applied irrigation at a rate of 10 mm 3 times at the beginning of the experiment. No fertilizer was applied to the plots.

Two plots (1 for each mixture) were mown for the measurements on 16 June 2016. The 2 other plots were mown on 29 June 2016.

2.2. Field Measurements

The 2 measurements, one on 16 June and the second on 29 June 2016 were made in 10 0.5 m × 0.5 m quadrats each containing 1 of the 2 mixtures. The quadrats were regularly distributed in the plots.

(a) Plenoptic images

The pictures were taken with a Lytro Illum. The Lytro company (Lytro inc Mountain View, CA, USA) no longer exists, but some cameras are still available, and a new plenoptic camera may be available for sale in the future. The Lytro Illum has 40 Megarays and produces images with a resolution of 1936 × 1290 pixels. The Lytro was positioned at a height of 1 m above the ground, with the lens aimed downward at the plant cover. The camera was fixed on a post inside the quadrat. The zoom was set at the minimum (30 mm).

In the Lytro Illum, a specific button (Lytro Button) can be used to select the different focus for the different objects in the picture. We used the Lytro Button to set the depth of image that adjusted the focused area; thus that the plant cover and the soil were each focused separately. The images were then exported to the Lytro desktop software (5.0 Lytro, inc, Mountain View, CA, USA) where they were processed to make net images (for each pixel, one focus was chosen, this focus was assumed by the software to be the one with the clearest images).

(b) Measurement of functional traits

In each quadrat, we randomly selected 2 individual representatives of all the sowed species and all the individuals of all the weed species. Three different functional traits were measured in each individual: plant height (H), leaf dry matter content (LDMC), and specific leaf area (SLA). Plant height is an indicator of the ability of the species to compete for light and of its seed dispersal ability [27]. H is the distance in m from the ground to the highest mature leaf stretched along with the stem of the individuals.

Leaf dry matter content (LDMC) is the ratio of leaf dry mass to fresh leaf mass expressed in $\text{mg}\cdot\text{g}^{-1}$. Specific leaf area (SLA) is the ratio of fresh leaf area to dry mass expressed in $\text{cm}^2\cdot\text{g}^{-1}$. Both traits are linked to the leaf economic spectrum (physiological and nutrient balance) [28]; both traits are linked to the growth strategy and the impact of the vegetation on the biogeochemical cycles. Following the standard protocol [29], we measured both traits using the uppermost mature leaf on the selected individual. The leaves were collected in the field in the morning and stored in cold, wet conditions, and scanned and weighed in the lab at the latest a few hours later. The leaves were then dried at 55 °C for 48 h to measure dry mass. The scan of the leaves was subsequently analyzed using WinFolia software [30].

(c) Biomass NIRS measurements and species composition

After these traits were measured, all the vegetation in the quadrat was mowed to a height of 5 cm.

NIRS measurements were taken with a LabSpec Pro (serial number 28,007). The lab specters had a spectral range of 350 to 2500 nm with a gap of 1 nm. The size of the captors was 3 cm. We acquired 40 different spectra of the fresh mass in each quadrat. Between each quadrat, we used a spectralon to calibrate the tools. We measured the fresh mass in each quadrat and then sorted the biomass per species. All the species that were not sown were classified as weed species. The fresh mass of the different groups was measured after which all the samples were dried at 55 °C for 48 h to determine their dry mass.

2.3. Images and NIRS Processing

The raw images from the Lytro Illum camera were processed to produce the totally clean images using the Lytro desktop software. We exported the images in tiff format. We also exported the depth map of the images. The depth map shows the focal points used to create clean images. For each pixel, the number of focal points used to produce the clean images is given on the image. Figure 1 is an example of a depth map together with the picture at the origin of this depth map.



Figure 1. Examples of Lytro photographs. (center) the fully focused image. (left) the depth map. (right) one example of segmentation (the soil is in yellow, *Trifolium alexandrinum*, is in red, *Viscia sativa* is in green).

We used 2 different approaches for the images:

- A segmentation approach to separate the images into different categories based on plant species. This enabled us to evaluate the extent of the cover of each species;
- A color approach to evaluate the greenness of the cover.

(a) Image segmentation

The aim of image segmentation was to separate the image into multiple sets of pixels based on one species. The first step in segmentation was to calculate a set of descriptors based on color, shape, and proximity on each pixel. The second step was to identify several pixels or groups of pixels for each species to use to train the algorithm. Finally, the algorithm was used on the remaining image to segment the images based on the training set.

We used the plug-in Trainable Weka Segmentation (TWS) of ImageJ software [31]. The algorithm used in TWS was a TreeForest classifier.

Regarding the different parameters in TWS software, we chose to use only the maximum and minimum among the possible descriptors. The training set in the image was a small square in the field that contained only one species.

First, we cropped the image thus that only the inside of the quadrat remained in the image. We masked the dark part of the image to remove images of the soil. There was one training set for each mixture. The algorithm trained on these 2 images was then applied to the other 19 images of the same mixtures.

However, we did not undertake segmentation of all the species; indeed, *Avena sativa* and *Medicago truncatula* did not grow well in the plots and were consequently not present in every quadrat. We carried out only one segmentation with the dominant species (i.e., *T. alexandrinum* for both mixtures, *V. sativa* for mixture 1 and *T. michelianum* for mixture 2) and the soil. The resulting classification enabled us to estimate the cover ratio between the different species for each studied plot that was used to predict field descriptors.

(b) Color Analysis

We calculated the mean value and the standard deviation for the different colors in the image (blue, red, and green canal) using the perfectly clean images and the cropped images, the different colors were coded from 0 to 255. We did the same with the depth map t, and the depths were also coded from 0 to 255. These variables were used to predict field descriptors. We did not correct the colors based on the light conditions but used the direct outputs from the camera.

(c) NIRS Analysis

The raw spectra were transformed using an SNV (standard normal variation) transformation followed by a linear DETREND.

For NIRS, for each wavelength between 1000 and 2500 nm, we calculated the average and the standard deviation of the 40 spectra per quadrat. With both these variables, we calculated the coefficient of variation as the ratio between the standard deviation and the mean value. To reduce these variables, we performed a Principal component analysis (PCA) of the average value per nm of the 40 quadrats, a PCA of the standard deviation per nm, and the coefficient of variation per nm. We used the two axes of each PCA as predictors.

2.4. Statistical Analysis

(a) Calculation of vegetation descriptors

We calculated different descriptors for field measurements: total fresh biomass, the biomass of each species, and the biomass of the unsown species (weeds). Functional diversity indices, CWM (community-weighted mean value), functional (FRic) and functional diversity (FD) using the Rao index was calculated for each trait separately. The indices were calculated using the FD package in Rcore Software [32].

Table 2 shows the distribution of the values of these vegetation descriptors across the 40 quadrats.

Table 2. Average value of the different vegetation characteristics. This table presents the overall average of the different variables of the vegetation and the average per plot (mix and cutting date).

	General Average	16 June		29 June	
		Mix1	Mix2	Mix1	Mix2
CWM. H in cm	42.67	40.84	32.29	48.07	49.49
CWM.LDMC in $\text{mg}\cdot\text{g}^{-1}$	336.68	322.32	287.05	345.51	391.83
CWM.SLA in $\text{cm}^2\cdot\text{g}^{-1}$	21.01	21.13	25.36	19.73	17.84
FRicH	1.70	1.82	2.06	1.45	1.45
FRicLDMC	1.68	2.66	1.41	0.97	1.69
FRicSLA	2.09	2.43	2.70	1.34	1.88
RaoQH	0.34	0.26	0.55	0.27	0.30
RaoQLDMC	0.41	0.51	0.26	0.21	0.68
RaoQSLA	0.53	0.49	0.66	0.25	0.70
Biomass in g	200.31	206.53	217.69	227.50	149.50
Ta biomass in g	120.95	100.56	129.23	153.00	101.00
Tm biomass in g	17.79	0.00	53.65	0.00	17.50
Mg biomass in g	0.04	0.05	0.10	0.00	0.00
Av biomass in g	8.30	4.28	5.91	9.50	13.50
Vc biomass in g	34.06	80.22	0.00	56.00	0.00
Weed biomass in g	23.91	13.75	25.89	21.50	34.50

- (b) Correlation between the different variables 2 by 2 using the maximum information coefficients

The first step was to analyze the correlation between the different descriptors of the vegetation and the different variables obtained from the plenoptic images and the NIRS. The links between these variables were not necessarily linear and were not necessarily well assessed using the standard Pearson correlation coefficient. The maximum information coefficient (MIC) is a correlation method that can be used to assess all types of relationships between two variables [33,34]. We calculated the MIC coefficient between all the vegetation descriptors and the images and NIRS variables using the Minerva package in R [35].

- (c) Evaluating the complementarity and redundancy between the variables using variance partitioning

We used variance partitioning [36] to evaluate complementarity between segmentation, color analysis, and NIRS. We assigned the different explanatory variables into three groups (variables resulting from the PCA on the NIRS, variables from color analysis, and variables from the segmentation). We performed variance partitioning for each of the field descriptors. We ran the variance partitioning using the varpart function in the vegan package [37].

- (d) Predicting capacity using partial least squares regression

We used a Partial Least Square (PLS) regression to quantify how much variance of the different vegetation descriptors can be predicted from the plenoptic images and NIRS variables. PLS regression was used to find relationships between 2 sets of variables. The 2 sets of variables were transformed into latent variables like in a PCA, except that the latent variables were not made to maximize the variances within the 2 sets but to maximize the relationships between the two sets of variables. PLS was thus appropriate for our dataset that contained numerous variables but a limited number of individuals (in this case only 40). The PLS was run with all the field descriptors combined. We used the function plsreg2 in the plsdeplot package in R.

3. Results

3.1. MIC Correlation

Table 3 lists the MIC correlation coefficients between the vegetation descriptors and the variables obtained using the plenoptic camera and the NIRS.

Table 3. Maximum correlation coefficient (MIC) between the vegetation descriptors and the NIRS variables (the color analysis of the image and the percentage extracted from the segmentation). The correlation coefficients in bold represent a significant correlation.

	NIRS							Colors					Segmentation					
	NIRSM1	NIRSM2	NIRSS1	NIRSS2	NIRSCV1	NIRSCV2	Vmdeep	Sddeep	VmR	SDR	VmB	SDB	VmG	SDG	TA	TM	VC	Soil
CWM. H	0.33	0.59	0.40	0.37	0.29	0.38	0.31	0.32	0.59	0.69	0.28	0.34	0.31	0.39	0.31	0.36	0.34	0.48
FRicH	0.27	0.28	0.32	0.33	0.22	0.21	0.37	0.25	0.34	0.41	0.24	0.46	0.25	0.37	0.39	0.25	0.26	0.39
RaoQH	0.26	0.33	0.25	0.34	0.18	0.31	0.30	0.33	0.31	0.41	0.24	0.26	0.22	0.21	0.31	0.28	0.28	0.49
CWM.LDMC	0.23	0.48	0.29	0.31	0.40	0.29	0.20	0.33	0.45	0.50	0.36	0.26	0.48	0.28	0.27	0.27	0.24	0.38
FRicLDMC	0.37	0.18	0.43	0.23	0.39	0.23	0.41	0.23	0.20	0.25	0.30	0.33	0.36	0.31	0.20	0.24	0.24	0.24
RaoQLDMC	0.33	0.20	0.29	0.23	0.48	0.22	0.61	0.32	0.28	0.31	0.26	0.24	0.32	0.31	0.25	0.19	0.19	0.26
CWM.SLA	0.25	0.36	0.36	0.28	0.30	0.28	0.27	0.17	0.38	0.37	0.39	0.26	0.30	0.28	0.31	0.28	0.28	0.28
FRicSLA	0.23	0.34	0.23	0.24	0.32	0.26	0.29	0.31	0.32	0.35	0.23	0.28	0.25	0.43	0.31	0.21	0.26	0.25
RaoQSLA	0.35	0.29	0.35	0.32	0.55	0.31	0.29	0.21	0.40	0.31	0.28	0.26	0.27	0.36	0.24	0.33	0.33	0.31
Biomass in g	0.55	0.30	0.20	0.36	0.37	0.30	0.31	0.21	0.45	0.43	0.22	0.23	0.24	0.22	0.57	0.48	0.35	0.39
Ta biomass in g	0.35	0.29	0.41	0.33	0.34	0.30	0.33	0.26	0.28	0.38	0.29	0.23	0.34	0.21	0.27	0.28	0.18	0.23
Tm biomass in g	0.31	0.46	0.32	0.28	0.32	0.28	0.21	0.29	0.53	0.50	0.30	0.32	0.22	0.34	0.53	1.00	1.00	0.78
Mg biomass in g	0.28	0.20	0.23	0.22	0.26	0.19	0.23	0.38	0.32	0.30	0.26	0.25	0.29	0.32	0.16	0.24	0.15	0.22
Av biomass in g	0.23	0.25	0.58	0.33	0.29	0.25	0.27	0.49	0.30	0.33	0.43	0.27	0.34	0.30	0.33	0.29	0.20	0.22
Vc biomass in g	0.28	0.35	0.32	0.31	0.22	0.34	0.22	0.29	0.53	0.41	0.20	0.32	0.30	0.34	0.41	1.00	1.00	0.77
Weed biomass in g	0.37	0.34	0.38	0.44	0.25	0.39	0.22	0.19	0.53	0.44	0.27	0.24	0.29	0.34	0.30	0.22	0.24	0.31

(a) Vegetation height descriptors

For the descriptors calculated with plant height, correlations were found with the standard deviation of the red canal obtained from the plenoptic images (0.69 for the CWMH and 0.41 for the FRiC and the Rao, respectively).

The CWM H was also linked with the average red canal (0.59), the second axis of the PCA on the NIRS average reflectance (0.59), and the percentage of soil extracted from the segmentation (0.48). FRiC H was linked with the standard deviation of the blue color in the plenoptic image (0.46). The Rao H was also linked with the evaluation of the soil percentage (0.49).

(b) Descriptors of leaf dry matter content

For the descriptors calculated with the LDMC, correlations were found between the CWM LDMC with the second axis of the PCA on the NIRS average reflectance (0.48) and with the first axis of the NIRS reflectance coefficient of variation (0.40), the average red value (0.45) and the standard deviation (0.50) of the red canal obtained from the plenoptic images. The CWM LDMC was also linked with the average green value obtained from the plenoptic images (0.48).

Both FRiC and Rao of LDMC were linked to the average deepness value (respectively, 0.41 and 0.61). Both descriptors were also linked with NIRS dimensions, with the first axis obtained from the standard deviation for the FRiC LDMC (0.43) and with the first axis obtained from the CV for the RaoLDMC (0.48).

(c) Descriptors of specific leaf area

The community weighted mean value of SLA was not linked to any variable. The FRiC SLA was linked with the standard deviation of the green color obtained from the plenoptic images only (0.43). The Rao SLA was linked with the first axis of the PCA for the coefficient of variation from the NIRS (0.55) and the average red value from the plenoptic images (0.40).

(d) Biomass and species composition

Total biomass was linked to the first axis of the PCA made with the average NIRS value (0.55), the average value, and the standard deviation of the red image (respectively 0.45 and 0.43). Total biomass was linked to the estimation of the biomass of *T. alexandrinum* and *T. michelianum* (0.57 and 0.48).

The biomass of *T. alexandrinum* was linked with the first axis of the PCA on the standard deviation of the NIRS spectra (0.41).

The biomass of *T. michelianum* was linked with the second axis of the average NIRS value (0.46), the average and the standard deviation of the red canal on the plenoptic images (0.53 and 0.50). The *T. michelianum* biomass was linked with all the variables obtained from the segmentation (estimation of soil cover, TM cover, TA cover).

The biomass of *Avena sativa* was linked with the first axis of the PCA on the standard deviation of the NIRS spectra (0.58), the standard deviation of the depth map (0.49), and the average value of the blue canal (0.43).

The *V. sativa* biomass was linked with the average and the standard deviation of the red canal from the plenoptic image (0.53 and 0.41) and with all the segmentation variables.

The weed biomass was linked with the second axis of the PCA on the standard deviation of NIRS (0.44 and the average and the standard deviation of the red canal from the plenoptic image (0.53 and 0.44).

3.2. Variance Partition

Table 4 presents the results of the variance partition. The first presented descriptors are those with the lowest residuals (highest variance), followed by the descriptors with the lowest explained variance.

Table 4. Results of variance partition. C corresponds to the variance explained by color analysis alone, S corresponds to the variance explained by segmentation alone, N corresponds to the variance explained by NIRS variables alone, CS corresponds to the joint variance between the colors and segmentation, SN corresponds to the joint variance between NIRS and segmentation, CN corresponds to the joint variance between NIRS and segmentation, and CSN is the variances explained by the three different groups combined. R corresponds to the unexplained variances (Residuals).

Field Variable	C	S	N	CS	SN	CN	CSN	R
CWM. H in cm	0.02	−0.05	0.07	0.01	0.06	0.08	0.19	0.63
CWM.LDMC in $\text{mg}\cdot\text{g}^{-1}$	0.00	−0.14	−0.15	0.05	0.09	0.17	0.03	0.96
CWM.SLA in $\text{cm}^2\cdot\text{g}^{-1}$	0.15	−0.07	0.09	0.00	0.03	0.10	0.06	0.63
FRicH	0.23	−0.01	0.13	−0.03	−0.10	−0.17	0.13	0.81
FRicLDMC	−0.02	−0.09	−0.10	0.01	0.08	0.09	−0.01	1.05
FRicSLA	0.00	0.02	0.05	0.05	−0.03	0.08	0.13	0.69
RaoQH	0.33	0.16	0.26	0.01	−0.19	−0.26	0.18	0.51
RaoQLDMC	0.08	−0.05	0.28	0.02	0.12	0.05	−0.15	0.65
RaoQSLA	−0.08	−0.02	0.06	0.07	0.04	0.03	−0.03	0.92
Biomass in g	0.07	0.04	−0.05	0.11	0.08	0.02	0.15	0.57
Ta biomass in g	−0.03	0.21	0.22	0.00	−0.09	0.06	−0.04	0.67
Tm biomass in g	0.19	0.29	0.08	−0.04	0.07	−0.09	0.27	0.25
Mg biomass in g	−0.05	0.06	0.01	−0.02	−0.03	0.19	−0.10	0.94
Av biomass in g	−0.21	−0.09	−0.11	0.05	0.11	0.10	0.06	1.08
Vc biomass in g	−0.07	0.29	0.07	−0.05	0.32	0.06	−0.02	0.41
Weed biomass in g	0.00	0.03	0.46	−0.02	0.03	0.15	−0.06	0.40

T. michelianum biomass was the descriptor with the lowest residuals (unexplained variance) with a value of 25%. The segmentation variables alone explained 29% of the variance of the *T. michelianum* biomass, 27% was explained by the combination of the three groups of variables (CSN), and 19% was explained by the color variables.

The second descriptor with lower residuals was weed biomass (residual 40%). The weed biomass was mostly explained by the NIRS variables (46%), thus by the combination of color analysis and NIRS (15%).

Vicia sativa biomass had 41% of residuals. The variance was explained by the segmentation variables (29%) and by the combination of segmentation and NIRS (32%).

RaoQH had 51% of residuals. The RaoQH was explained by color variables alone (33%), NIRS alone (26%), the combination of the three groups of variables (18%) and segmentation alone (16%).

Total biomass had 57% of residuals. The combination of the three groups of variables explained 15% of the variance (CSN), and 11% was explained by the combination of color analysis and segmentation.

A total of 63% of CWM H variance remained unexplained in the variance partition; 19% of the variance was explained by the combination of the three groups of variables.

A total of 37% of CWM SLA variance was explained, 15% of the variance was explained by the color variables alone, and 10% of the variance by the combination of the color analysis and the NIRS variables.

A total of 35% of RaoQLDMC variance was explained by the different variables. The NIRS variables alone explained 28% of the variance.

A total of 33% of *Trifolium alexandrium* biomass variance was explained by the set of variables. NIRS only explained 22% of the variance of *Trifolium alexandrium* biomass.

The FriCSLA had 69% of residuals. The combination of the three groups of variables explained 13% of the variance.

The other vegetation descriptors had more than 80% of residuals.

3.3. Partial Least Squares (PLS) Regressions

Figure 2 presents the results of the PLS. The first axis t1 was positively defined by the standard deviation of the three colors obtained from the image and the average red color.

The first axis was also linked with the PCA obtained from the NIRS spectra (positively with the first axis of the PCA on the standard deviation and the first axis on the coefficient of variation, the second on the average spectrum; negatively with the second axis made on the coefficient of variation and the standard deviation). The second axis t_2 was mainly defined by the segmentation variable (positively with the soil and *Vicia sativa* percentage evaluation) and negatively with the percentage evaluation of *T. michelianum*.

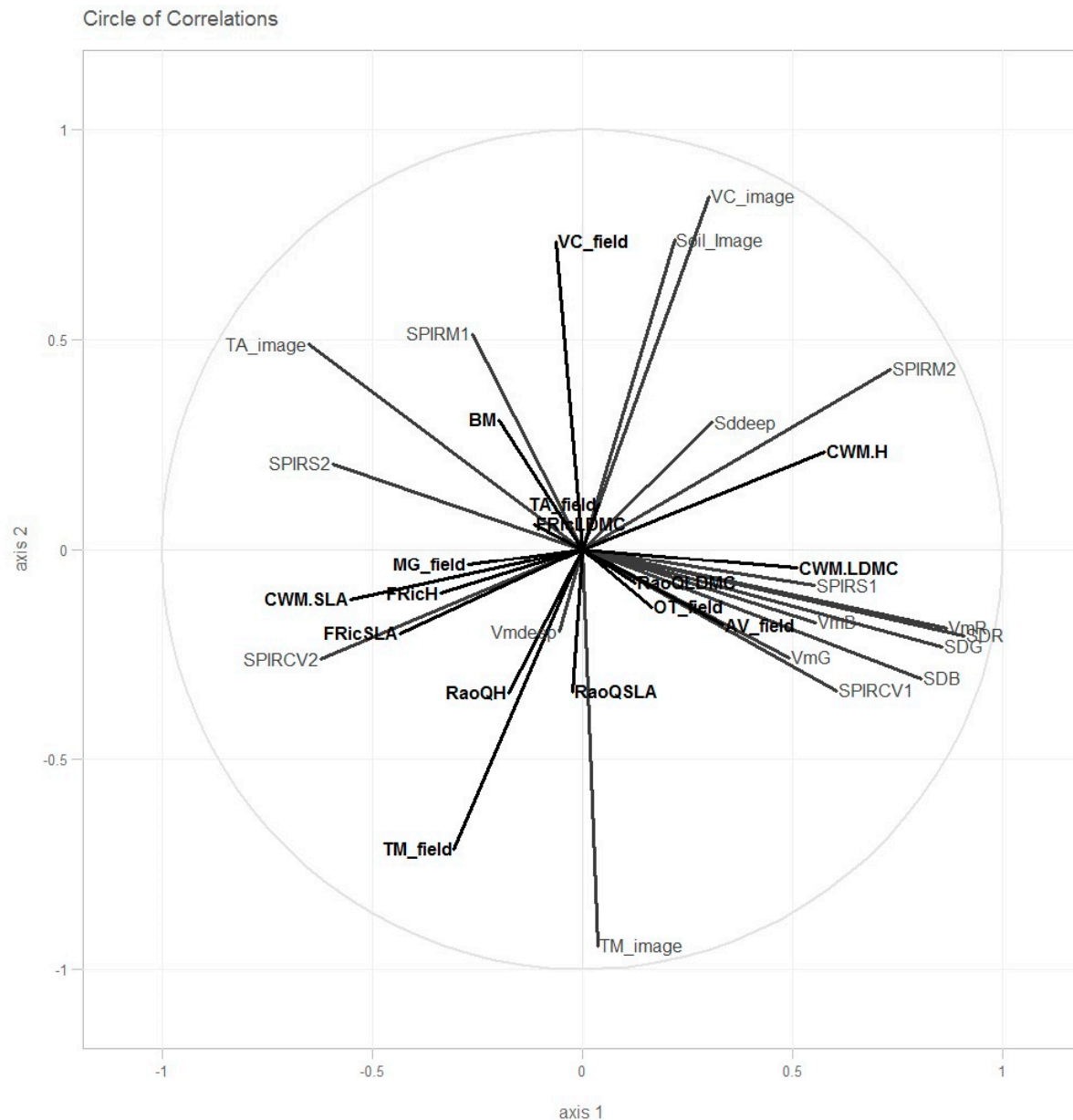


Figure 2. Correlation circle of PLS regression. The vegetation descriptors measured in the field are in black and the variables obtained from the plenoptic image and NIRS are in gray.

Table 5 presents the Q^2 for each vegetation descriptor. The CWM variables were linked with the first axis, positively for the H ($Q^2 = 0.24$) and the LDMC ($Q^2 = 0.20$) and negatively for the SLA ($Q^2 = 0.24$). The FRic SLA was also negatively linked with the first axis ($Q^2 = 0.16$).

Table 5. Results of the PLS.Q² on the two first latent variables for the different vegetation descriptors.

	t1	t2
CWM. H in cm	0.244	0.014
CWM.LDMC in mg·g ⁻¹	0.200	−0.064
CWM.SLA in cm ² ·g ⁻¹	0.242	−0.049
FRicH	0.071	−0.039
FRicLDMC	−0.019	0.050
FRicSLA	−0.012	−0.054
RaoQH	−0.011	−0.115
RaoQLDMC	0.155	0.007
RaoQSLA	−0.053	0.012
Biomass in g	−0.046	0.035
Ta biomass in g	−0.083	−0.044
Tm biomass in g	0.022	0.512
Mg biomass in g	0.010	−0.090
Av biomass in g	0.063	−0.029
Vc biomass in g	−0.020	0.511
Weed biomass in g	−0.018	−0.024
Q ²	0.047	0.043

T. michelianum biomass was negatively linked with the second axis of the PLS ($Q^2 = 0.51$) and *Vicia sativa* biomass was positively linked with the same axis ($Q^2 = 0.51$).

4. Discussion

4.1. Limits of This First Attempt

This original work is a first attempt to combine the use of plenoptic cameras and NIRS to monitor grassland vegetation. This study has some serious limits and cannot yet be generalized.

Our mixtures were not as successful as planned, which limited our results. Our main problem was the establishment of the grassland: only three of the five sowed species grew in our plots and only two species were present in each mixture (*T. alexandrinum* and *V. sativa* in the first mixture and *T. alexandrinum* and *T. michelianum* in the second one). One of the reasons was the delayed establishment of the grassland (middle of April). In fact, we sowed the mixtures in October of the previous year of the measurements (2015) but all the seeds were removed by a flood just after sowing. We consequently had to sow a second batch in April. This late sowing also shortened the period in which measurements were possible. In such Mediterranean mixtures, the vegetation is usually green from March to June. Due to late sowing, the mixtures were only green in May and June. Our original plan was to mow twice to increase the number of measurements. However, none of the species grew after the first cut. Since our budget only covered a one-year experiment we were not able to continue in the following year. As a result, we only had data from 40 quadrats to work with.

As we are well aware of the limits of this first study, we do not present this work as a tool ready to be used but to pave the way for further research on the development of this new tool. We think that this work has several originalities and that the research community will be interested in these preliminary results.

4.2. Evaluating Functional Traits and Diversity Using Optical Captors

Until today, very few studies have attempted to assess functional traits using optical tools [16,38]. These traits have been directly linked with the different plant functions, including reproduction, growth, and survival of the plant [6]. For example, the SLA and the LNC (leaf nitrogen content) are soft trait indicators of photosynthesis [28]. Functional traits are generally used as indicators of more complex functions. However, collecting and measuring functional traits are laborious: for most traits, at least five individuals of each species have to be collected, but at least 10 individuals are recommended (or even 25 for

some traits) per species (see the first appendix of standard protocols [29] for more details). In highly diverse ecosystems, the collection of all these individuals is quite an undertaking. Some authors suggest only collecting the dominant species, i.e., those that represent up to 80% of the biomass [39]. Others propose using a random individuals approach instead of the species approach by sampling only 20 individuals in the field irrespective of the species [40]. In both cases, low abundance species are not sampled. The absence of these species could be problematic in the calculation of functional diversity [41] and for the studies of ecosystem functions [42–44]. Instead of field measurements, it is possible to use a functional trait database, but this is also problematic [45].

Another limitation of measuring functional traits is that it is destructive, meaning it is difficult to complete monitoring in only one season.

Our work, which is only based on three functional traits and on three different functional diversity indices, did reveal some correlations (Table 3) between these indices and outputs from the camera and the NIRS. These weighted mean values of the SLA and the LDMC of these communities were linked with the colors obtained from the plenoptic camera and with the NIRS PCA variables. SLA and LDMC are two traits linked to the leaf-economic spectrum. [28]. Species with a high SLA and low LDMC are generally associated with high photosynthesis rates and high nitrogen content (due to the high Rubisco content) [28,46,47]. Conversely, plants with a low SLA and high LDMC are associated with low nitrogen content and low photosynthetic activity but also with hard tissues and more secondary metabolites, especially for defense against herbivory. Nitrogen content, dry matter content, some secondary metabolites, and hard tissues are generally well assessed by NIRS [48].

Our work also shows that the standard deviation (and the coefficient of variation) of the 40 spectra per quadrat can be used for the assessment of vegetation descriptors and not only the mean value.

Based on variance partition, we saw that the colors obtained from the plenoptic image were equivalent to the information obtained with the NIRS.

The community weighed mean value of plant height (CWMH) was also linked with the NIRS data and with the red canal obtained from the plenoptic images. Similar results were also found for the leaf economic spectrum traits. The CWM H is known to be linked with the leaf economic spectrum [49]. The link between NIRS and height may thus be indirect via leaf physiology. Moreover, we harvested on two dates in our experiment. At the date of the second and last harvest (29 June), the plants were taller but had a lower SLA and higher LDMC. These differences could be due to the difference in phenological stages, which might mean that NIRS and color analysis could also be used to evaluate the phenology of the grassland. Our work show interest in using optical tools for the evaluation of functional trait and diversity.

4.3. Future Outlook on the Use of Plenoptic Images

In this work, we used a plenoptic camera to take advantage of the clean images and the associated depth map only. In our plots, the grass was not very tall (maximum 50 cm); hence, the interest of using plenoptic was less than it would be with taller species with different vegetative strata. Indeed, in the case of a plant cover less than 50 cm tall, it may be possible to obtain a clean picture with a classical digital camera.

The potential advantage of using a depth map is to evaluate the vertical heterogeneity of the cover. However, we found no correlation between the average value and the standard deviation of the depth map and any vegetation descriptors. The depth map could be more useful for more heterogeneous vegetation.

One of our hypotheses in this work was that a clean image would enable a better image analysis. However, blurring the images can help image analysis. Indeed, blurring could provide information about the distance between the objects and the camera; some objects, such as the soil as well as small species, may only be in the background. One could imagine a segmentation algorithm using not only the clean image but also the depth

map such as a digital surface model (DSM) and possibly all the pictures obtained at all the different focuses [50]. Indeed, some authors have used the numerical surface model to improve segmentation [51]. We compared the results of the segmentations made with a clean picture, a picture with a focus on the background, and another picture with the focus on the aboveground part of the vegetation. The results of the segmentations were quite different (results not shown). It may be interesting to use different images with different focuses for image analysis.

Thanks to the presence of multiple captors in the camera lens, plenoptic cameras can also produce a 3D image. The difference in the views taken from these lenses are used to produce a 3D image. This 3D image is not complete and does not cover all the directions, but 3D imaging is a promising tool for evaluating vegetation [52]. A 3D image could be produced by a 3D camera but also based on the structure of motion [53]. Structure from motion is generally used from UAV but some studies have shown that the same process could be used for grass with a simple digital camera [54].

4.4. Combination of Several Tools

One part of the information captured by the color analysis was also captured by the NIRS (Table 4 and Figure 2) for most of the vegetation descriptors. However, the information captured by the two approaches differs in some criteria (e.g., RaoQH). Nevertheless, the two tools can be used for different purposes. The camera is easier to use in the field and less costly; it could be used to obtain a rapid but less accurate assessment in the field. NIRS tools (in our case, the ASD LabSpec) could evaluate functional traits more accurately, but for the moment, this approach is more expensive and less field-friendly.

Furthermore, unlike the camera, NIRS does not produce spatial information. Hyperspectral imagery is one possible way to obtain both spectral and spatial details [55]. Hyperspectral information could also be useful for segmentation.

The segmentation approach complemented NIRS and color analysis (Figure 2) and explained more variability for some vegetation descriptors, particularly to estimate the biomass of the different species. Combining the two types of procedures and images could be an advantage when evaluating a large panel of descriptors (the camera with segmentation for the species composition, NIRS, and color analysis for the functional traits and diversity descriptors).

Other tools can also be used to obtain a better grasp of grassland (Laser, LIDAR, Ultrasound) [10]. A recent study shows that a combination of several captors is more accurate than only one captor [56].

5. Conclusions

This work was the first attempt to use plenoptic cameras for the evaluation of grassland vegetation descriptors. It is one of the first assessments using a plenoptic camera for grassland studies. Plenoptic cameras could be very useful for producing clean images and a set of images with different focuses. However, our work was limited by the low diversity in our mixtures (only two main species per mixture). The height of the vegetation resulting from the mixture was not sufficient to allow the evaluation of the full potential of the plenoptic camera. We were not able to evaluate more than 50% of the field variability only for three variables. These tools cannot be, for the moment, used for prediction.

We also tested the interest of combining NIRS data with camera pictures. NIRS can produce similar information to that obtained from color analysis of the plenoptic images. Not only the average value of the NIRS spectrum but also the standard deviation could be useful for the assessment of the plant cover. Different combinations of tools now need to be tested.

Author Contributions: Conceptualization, S.T. and L.J. and P.B.; Methodology, S.T., F.B., P.B. and L.J.; Software, F.B., P.B. and M.L. (Matthieu Lesnoff); Formal Analysis, M.D. and M.L. (Matthieu Lesnoff); Investigation, M.L. (Mylène Lascoste) and J.M.C.; Resources, J.M.C. and M.L. (Mylène Lascoste); Data Curation, M.L. (Mylène Lascoste) and M.D.; Writing—Original Draft Preparation, S.T.; Writing—Review and Editing, S.T., M.D., M.L. (Mylène Lascoste), M.L. (Matthieu Lesnoff), F.B., P.B. and L.J.; Visualization, S.T.; Supervision, S.T. and L.J.; Project Administration, S.T. and L.J.; Funding Acquisition S.T. All authors have read and agreed to the published version of the manuscript.

Funding: The Research was funded by CIRAD within the AI CRESI “plénoherbe”.

Institutional Review Board Statement: Not applicable.

Informed Consent Statement: Not applicable.

Conflicts of Interest: The authors declare no conflict of interest.

References

1. Panunzi, E. *Are Grasslands under Threat? Brief Analysis of FAO Statistical Data on Pasture and Fodder Crops*; UN Food and Agriculture Organization: Rome, Italy, 2008.
2. Givens, D.I.; Owen, E.; Omed, H.; Axford, R. *Forage Evaluation in Ruminant Nutrition*; CABI: Wallingford, UK, 2000.
3. Van Soest, P.J.; Robertson, J.B.; Lewis, B.A. Methods for dietary fiber, neutral detergent fiber, and nonstarch polysaccharides in relation to animal nutrition. *J. Dairy Sci.* **1991**, *74*, 3583–3597. [\[CrossRef\]](#)
4. McMahon, L.R.; McAllister, T.A.; Berg, B.P.; Majak, W.; Acharya, S.N.; Popp, J.D.; Coulman, B.E.; Wang, Y.; Cheng, K.-J. A review of the effects of forage condensed tannins on ruminal fermentation and bloat in grazing cattle. *Can. J. Plant Sci.* **2000**, *80*, 469–485. [\[CrossRef\]](#)
5. Spiegelberger, T.; Gillet, F.; Amiaud, B.; Thébault, A.; Mariotte, P.; Buttler, A. How do plant community ecologists consider the complementarity of observational, experimental and theoretical modelling approaches? *Plant Ecol. Evol.* **2012**, *145*, 4–12. [\[CrossRef\]](#)
6. Violle, C.; Navas, M.-L.; Vile, D.; Kazakou, E.; Fortunel, C.; Hummel, I.; Garnier, E. Let the concept of trait be functional! *Oikos* **2007**, *116*, 882–892. [\[CrossRef\]](#)
7. Schleuter, D.; Daufresne, M.; Massol, F.; Argillier, C. A user’s guide to functional diversity indices. *Ecol. Monogr.* **2010**, *80*, 469–484. [\[CrossRef\]](#)
8. McGill, B.J.; Enquist, B.; Weiher, E.; Westoby, M. Rebuilding community ecology from functional traits. *Trends Ecol. Evol.* **2006**, *21*, 178–185. [\[CrossRef\]](#) [\[PubMed\]](#)
9. De Bello, F.; Lavorel, S.; Díaz, S.; Harrington, R.; Cornelissen, J.H.C.; Bardgett, R.D.; Berg, M.P.; Cipriotti, P.; Feld, C.K.; Hering, D.; et al. Towards an assessment of multiple ecosystem processes and services via functional traits. *Biodivers. Conserv.* **2010**, *19*, 2873–2893. [\[CrossRef\]](#)
10. Wachendorf, M.; Fricke, T.; Möckel, T. Remote sensing as a tool to assess botanical composition, structure, quantity and quality of temperate grasslands. *Grass Forage Sci.* **2018**, *73*, 1–14. [\[CrossRef\]](#)
11. Rouse, J.W.; Haas, R.H.; Schell, J.A.; Deering, D.W. Monitoring vegetation systems in the great plains with ERTS. In Proceedings of the Third ERTS Symposium, SP-351, Washington, DC, USA, 10–14 December 1973.
12. Chen, J.; Gu, S.; Shen, M.; Tang, Y.; Matsushita, B. Estimating aboveground biomass of grassland having a high canopy cover: An exploratory analysis of in situ hyperspectral data. *Int. J. Remote Sens.* **2009**, *30*, 6497–6517. [\[CrossRef\]](#)
13. Mutanga, O.; Skidmore, A. Integrating imaging spectroscopy and neural networks to map grass quality in the Kruger National Park, South Africa. *Remote Sens. Environ.* **2004**, *90*, 104–115. [\[CrossRef\]](#)
14. De Boever, J.; Cottyn, B.; Vanacker, J.; Boucqué, C. The use of NIRS to predict the chemical composition and the energy value of compound feeds for cattle. *Anim. Feed Sci. Technol.* **1995**, *51*, 243–253. [\[CrossRef\]](#)
15. Wachendorf, M.; Ingwersen, B.; Taube, F. Taube Prediction of the clover content of red clover- and white clover-grass mixtures by near-infrared reflectance spectroscopy. *Grass Forage Sci.* **1999**, *54*, 87–90. [\[CrossRef\]](#)
16. Pilon, R.; Klumpp, K.; Carrère, P.; Picon-Cochard, C. Determination of Aboveground Net Primary Productivity and Plant Traits in Grasslands with Near-Infrared Reflectance Spectroscopy. *Ecosystems* **2010**, *13*, 851–859. [\[CrossRef\]](#)
17. Bonnal, L.; Julien, L.; Delalande, M.; Bastianelli, D. How can a dry forage database be used to predict fresh grass composition by NIR spectroscopy? Data transfer vs. spectra transfer. In Proceedings of the International Conference on Near Infrared Spectroscopy, La Grande-Motte, France, 2–7 June 2013; pp. 685–688.
18. Onyango, C.; Marchant, J.; Grundy, A.; Phelps, K.; Reader, R. Image Processing Performance Assessment Using Crop Weed Competition Models. *Precis. Agric.* **2005**, *6*, 183–192. [\[CrossRef\]](#)
19. Hague, T.; Tillett, N.D.; Wheeler, H. Automated Crop and Weed Monitoring in Widely Spaced Cereals. *Precis. Agric.* **2006**, *7*, 21–32. [\[CrossRef\]](#)
20. Gebhardt, S.; Kühbauch, W. A new algorithm for automatic *Rumex obtusifolius* detection in digital images using colour and texture features and the influence of image resolution. *Precis. Agric.* **2007**, *8*, 1–13. [\[CrossRef\]](#)

21. Gebhardt, S.; Schellberg, J.; Lock, R.; Kühbauch, W. Identification of broad-leaved dock (*Rumex obtusifolius* L.) on grassland by means of digital image processing. *Precis. Agric.* **2006**, *7*, 165–178. [\[CrossRef\]](#)
22. Himstedt, M.; Fricke, T.; Wachendorf, M. Determining the Contribution of Legumes in Legume-Grass Mixtures Using Digital Image Analysis. *Crop Sci.* **2009**, *49*, 1910–1916. [\[CrossRef\]](#)
23. Himstedt, M.; Fricke, T.; Wachendorf, M. The Relationship between Coverage and Dry Matter Contribution of Forage Legumes in Binary Legume-Grass Mixtures. *Crop Sci.* **2010**, *50*, 2186–2193. [\[CrossRef\]](#)
24. Ng, R.; Levoy, M.; Brédif, M.; Duval, G.; Horowitz, M.; Hanrahan, P. *Light Field Photography with a Hand-Held Plenoptic Camera*; Computer Science Tech Report CSTR 2005-02; Stanford University: Stanford, CA, USA, 2005; pp. 1–11.
25. Hahne, C.; Aggoun, A.; Velisavljevic, V.; Fiebig, S.; Pesch, M. Refocusing distance of a standard plenoptic camera. *Opt. Express* **2016**, *24*, 21521–21540. [\[CrossRef\]](#)
26. Huguenin, J.; Julien, L.; Capron, J.; Desclaux, D.; Lesnoff, M.; Crespo, D. Multispecies pastures in Mediterranean zones: Agro-ecological resilience of forage production subject to climatic variations. *Grassl. Resour. Extensive Farming Syst. Marg. Lands Major Driv. Future Scenar.* **2017**, *2017*, 566–569.
27. Westoby, M. A leaf-height-seed (LHS) plant ecology strategy scheme. *Plant Soil* **1998**, *199*, 213–227. [\[CrossRef\]](#)
28. Wright, I.J.; Reich, P.B.; Westoby, M.; Ackerly, D.D.; Baruch, Z.; Bongers, F.; Cavender-Bares, J.; Chapin, T.; Cornelissen, J.H.C.; Diemer, M.; et al. The worldwide leaf economics spectrum. *Nature* **2004**, *428*, 821–827. [\[CrossRef\]](#)
29. Pérez-Harguindeguy, N.; Díaz, S.; Garnier, E.; Lavorel, S.; Poorter, H.; Jaureguiberry, P.; Bret-Harte, M.S.; Cornwell, W.K.; Craine, J.M.; Gurvich, D.E.; et al. New handbook for standardised measurement of plant functional traits worldwide. *Aust. J. Bot.* **2013**, *61*, 167–234. [\[CrossRef\]](#)
30. WinFolia, version PRO 2001; Regent Instruments Inc.: Quebec, QC, Canada, 2001.
31. Arganda-Carreras, I.; Kaynig, V.; Rueden, C.; Eliceiri, K.W.; Schindelin, J.; Cardona, A.; Seung, H.S. Trainable Weka Segmentation: A machine learning tool for microscopy pixel classification. *Bioinformatics* **2017**, *33*, 2424–2426. [\[CrossRef\]](#)
32. Laliberté, E.; Legendre, P.; Shipley, B. Package FD: Measuring Functional Diversity from Multiple Traits, and Other Tools for Functional Ecology. 2014. Available online: <https://cran.r-project.org/web/packages/FD/index.html> (accessed on 13 April 2022).
33. Reshef, D.N.; Reshef, Y.A.; Finucane, H.K.; Grossman, S.R.; McVean, G.; Turnbaugh, P.J.; Lander, E.S.; Mitzenmacher, M.; Sabeti, P.C. Detecting Novel Associations in Large Data Sets. *Science* **2011**, *334*, 1518–1524. [\[CrossRef\]](#)
34. Speed, T. A Correlation for the 21st Century. *Science* **2011**, *334*, 1502–1503. [\[CrossRef\]](#)
35. Albanese, D.; Filosi, M.; Visintainer, R.; Riccadonna, S.; Jurman, G.; Furlanello, C. Minerva and minepy: A C engine for the MINE suite and its R, Python and MATLAB wrappers. *Bioinformatics* **2013**, *29*, 407–408. [\[CrossRef\]](#)
36. Borcard, D.; Legendre, P.; Drapeau, P. Partialling out the Spatial Component of Ecological Variation. *Ecology* **1992**, *73*, 1045–1055. [\[CrossRef\]](#)
37. Oksanen, J.; Blanchet, G.; Kindt, R.; Legendre, P.; Minchin, P.; O'Hara, R.B.; Simpson, G.L.; Solymos, P.; Stevens, M.H.H.; Wagner, H. Vegan: Community Ecology Package. 2012. Available online: <https://cran.r-project.org/web/packages/vegan/index.html> (accessed on 13 April 2022).
38. Costa, F.R.C.; Lang, C.; Almeida, D.R.A.; Castilho, C.V.; Poorter, L. Near-infrared spectrometry allows fast and extensive predictions of functional traits from dry leaves and branches. *Ecol. Appl.* **2018**, *28*, 1157–1167. [\[CrossRef\]](#)
39. Garnier, E.; Cortez, J.; Billès, G.; Navas, M.-L.; Roumet, C.; Debussche, M.; Laurent, G.; Blanchard, A.; Aubry, D.; Bellmann, A.; et al. Plant Functional Markers Capture Ecosystem Properties during Secondary Succession. *Ecology* **2004**, *85*, 2630–2637. [\[CrossRef\]](#)
40. Lavorel, S.; Grigulis, K.; McIntyre, S.; Williams, N.S.G.; Garden, D.; Dorrough, J.; Berman, S.; Quétier, F.; Thébault, A.; Bonis, A. Assessing functional diversity in the field. *Methodol. Matters Funct. Ecol.* **2008**, *22*, 134–147.
41. Pakeman, R.; Quested, H. Sampling plant functional traits: What proportion of the species need to be measured? *Appl. Veg. Sci.* **2007**, *10*, 91–96. [\[CrossRef\]](#)
42. Walker, B.; Kinzig, A.; Langridge, J. Original Articles: Plant Attribute Diversity, Resilience, and Ecosystem Function: The Nature and Significance of Dominant and Minor Species. *Ecosystems* **1999**, *2*, 95–113. [\[CrossRef\]](#)
43. Mouillot, D.; Bellwood, D.R.; Baraloto, C.; Chave, J.; Galzin, R.; Harmelin-Vivien, M.; Kulbicki, M.; Lavergne, S.; Lavorel, S.; Mouquet, N.; et al. Rare Species Support Vulnerable Functions in High-Diversity Ecosystems. *PLoS Biol.* **2013**, *11*, e1001569. [\[CrossRef\]](#) [\[PubMed\]](#)
44. Violle, C.; Thuiller, W.; Mouquet, N.; Munoz, F.; Kraft, N.J.; Cadotte, M.W.; Livingstone, S.; Mouillot, D. Functional Rarity: The Ecology of Outliers. *Trends Ecol. Evol.* **2017**, *32*, 356–367. [\[CrossRef\]](#) [\[PubMed\]](#)
45. Violle, C.; Borgh, B.; Choler, P. Trait databases: Misuses and precautions. *J. Veg. Sci.* **2015**, *26*, 826–827. [\[CrossRef\]](#)
46. Wright, I.J.; Reich, P.B.; Cornelissen, J.H.C.; Falster, D.S.; Garnier, E.; Hikosaka, K.; Lamont, B.B.; Lee, W.; Oleksyn, J.; Osada, N.; et al. Assessing the generality of global leaf trait relationships. *New Phytol.* **2005**, *166*, 485–496. [\[CrossRef\]](#)
47. Wright, I.J.; Reich, P.B.; Cornelissen, J.H.C.; Falster, D.S.; Groom, P.K.; Hikosaka, K.; Lee, W.; Lusk, C.H.; Niinemets, Ü.; Oleksyn, J.; et al. Modulation of leaf economic traits and trait relationships by climate. *Glob. Ecol. Biogeogr.* **2005**, *14*, 411–421. [\[CrossRef\]](#)
48. Tran, H.; Salgado, P.; Lecomte, P. Species, climate and fertilizer effects on grass fibre and protein in tropical environments. *J. Agric. Sci.* **2009**, *147*, 555–568. [\[CrossRef\]](#)
49. Navas, M.-L.; Roumet, C.; Bellmann, A.; Laurent, G.; Garnier, E. Suites of plant traits in species from different stages of a Mediterranean secondary succession. *Plant Biol.* **2010**, *12*, 183–196. [\[CrossRef\]](#) [\[PubMed\]](#)

50. Prošek, J.; Šimová, P. UAV for mapping shrubland vegetation: Does fusion of spectral and vertical information derived from a single sensor increase the classification accuracy? *Int. J. Appl. Earth Obs. Geoinf.* **2019**, *75*, 151–162. [[CrossRef](#)]
51. Waser, L.; Baltsavias, E.; Ecker, K.; Eisenbeiss, H.; Feldmeyer-Christe, E.; Ginzler, C.; Küchler, M.; Zhang, L. Assessing changes of forest area and shrub encroachment in a mire ecosystem using digital surface models and CIR aerial images. *Remote Sens. Environ.* **2008**, *112*, 1956–1968. [[CrossRef](#)]
52. Aasen, H.; Burkart, A.; Bolten, A.; Bareth, G. Generating 3D hyperspectral information with lightweight UAV snapshot cameras for vegetation monitoring: From camera calibration to quality assurance. *ISPRS J. Photogramm. Remote Sens.* **2015**, *108*, 245–259. [[CrossRef](#)]
53. Frey, J.; Kovach, K.; Stemmler, S.; Koch, B. UAV Photogrammetry of Forests as a Vulnerable Process. A Sensitivity Analysis for a Structure from Motion RGB-Image Pipeline. *Remote Sens.* **2018**, *10*, 912. [[CrossRef](#)]
54. Bossoukpe, M.; Ndiaye, O.; Diatta, S.; Diatta, O.; Diouf, A.A.; Assouma, M.H.; Faye, E.; Taugourdeau, S. Ground based photogrammetry to assess herbaceous biomass in Sahelian rangelands. In Proceedings of the European Grassland Federation, Helsinki, Finland, 19–21 October 2020.
55. Dale, L.-M. L'utilisation de la spectrométrie (NIR) et l'imagerie hyperspectrale (NIR-HIS) proche infrarouge pour étudier la composition chimique et botanique de des fourrages. Ph.D. Thesis, Université of Liege, Liege, Belgique, 2014.
56. Moeckel, T.; Safari, H.; Reddersen, B.; Fricke, T.; Wachendorf, M. Fusion of Ultrasonic and Spectral Sensor Data for Improving the Estimation of Biomass in Grasslands with Heterogeneous Sward Structure. *Remote Sens.* **2017**, *9*, 98. [[CrossRef](#)]